JOURNAL OF CATALYSIS 133, 159–169 (1992)

Isomorphous Substitution of Iron Ions into Aluminophosphate Molecular Sieve, $AlPO_4$-5

JONG WOOK PARK AND HAKZE CHON

Department of Chemistry, Korea Advanced Institute of Science and Technology, P.O. Box 150, Cheongryang-Ni, Seoul 130-650, Korea

Received February 19, 1991; revised June 20, 1991

FAPO-5 molecular sieves synthesized with Fe(II) and TEAOH and differing in iron content have been characterized by using various physicochemical methods to elucidate the incorporation of the iron ions into the aluminophosphate matrix. In as-synthesized FAPO-5, a large portion of Fe(III) ions are located in the framework position of $AlPO_4$-5, and Fe(II) ions are introduced in place of Al(III) ions in the form of $Fe(II)TEA^+$. Fe(II) ions are oxidized to Fe(III) while remaining in the framework position in the course of calcination to remove the template. In the case of Fe-silicate ZSM-5, some of the Fe(III) ions located in the framework seem to be removed after the calcination.

INTRODUCTION

Recent advances in the area of heteroatom substituted aluminosilicate and aluminophosphate ($AlPO_4$) molecular sieves have opened a new area in zeolite catalysis (*1, 2*). Especially, considerable interest has been centered on the isomorphous substitution of iron into various molecular sieve zeolites (*3–15*). Several studies concerning the iron-incorporated aluminophosphate molecular sieve (FAPO) have recently been reported (*12–15*). FAPO material has been shown to modify the acidity of $AlPO_4$ and has potential applications as a catalyst for hydrocarbon conversion and oxidative combusion reactions (*16, 18*).

In the present study, the possibility of the isomorphous substitution of iron into an $AlPO_4$-5 matrix has been investigated with the help of various physicochemical methods.

EXPERIMENTAL

Sample Preparation

FAPO-5 samples were synthesized by the method described by C. A. Messina *et al.* (*16*) using pseudoboehmite (74.2 wt%, Conoco), $FeCl_2$ (Kanto, EP), H_3PO_4 (Kanto, 85%), and TEAOH (Aldrich, 40%). Pseudoboehmite was added slowly to H_3PO_4 solution with vigorous stirring until a homogeneous gel was obtained. Then $FeCl_2 \cdot 4H_2O$ was added to the gel with continuous stirring, followed by a dropwise addition of the organic templating agent (TEAOH). The pH of the final gel was 3.5–3.8. A gel with the molar composition 1.0 TEAOH:$x$$Fe_2O_3$:(1 − x) Al_2O_3:1.0 P_2O_5:80H_2O with x = 0, 0.02, 0.04, 0.06, and 0.08 was hydrothermally crystallized in a teflon-lined autoclave (250 ml) at 430 K for 70–80 hr. The samples are designated as F0, F1, F2, F3, and F4, respectively. Fe-silicate ZSM-5 for a comparison study was prepared by the method described by R. Szostak and T. L. Thomas (*3*) having a Si/Fe mole ratio of 65. The samples were filtered, washed, and dried at 400 K for 24 hr and kept in an as-synthesized form. The calcined form was prepared by flowing N_2 at 780 K for 5 hr, followed by flowing air at the same temperature for 5 hr.

Characterization

X-ray diffraction patterns were obtained with a Rigaku Ru-200B X-ray analyzer. The morphologies of the samples were observed

0021-9517/92 $3.00

with an ISISX-30E scanning electron microscope. Adsorption capacities of N_2, *n*-hexane, and benzene at 295 K and of 1,3,5-trimethylbenzene (TMB) at 363 K were obtained with a volumetric adsorption unit (*19*). The chemical analysis was performed by a combination of wet analysis, atomic absorption, and ICP methods. The surface compositions were determined by X-ray photoelectron spectroscopy (XPS, VG Scientific XPSLAB MK-2). The electron paramagnetic resonance (EPR) spectra were obtained with a Varian E-4 electron spin resonance spectrometer at room temperature or liquid nitrogen temperature using DPPH as standards. The relative intensity measurement of the $g = 4.3$ signal was made by integrating the derivative curve twice and comparing the result with a total integration of the spectrum. The photoacoustic (PA) spectra were obtained using a home-made PA spectrometer system (*20*). TGA/DTG and DSC were performed using a Rigaku Thermal Analyzer Station TAS-100 in the range 303–873 K by heating the sample (20–25 mg) at a rate of 5 K/min in an air or nitrogen flow. The temperature programmed decomposition (TPDE) measurements were conducted using a microcatalytic reactor attached to a quadrupole mass spectrometer (Finnigan 400). The catalysts (~100 mg) were placed in a quartz tubular microreactor (O.D. = 11 mm) and heated at a rate of 6 K/min in a helium (Matheson, 99.999%) flow of 160 ml/min. The products were passed through a jet separator and introduced by way of a Granville Phillips variable leak valve into the mass spectrometer.

RESULTS

Figure 1 shows the XRD patterns of as-synthesized $AlPO_4-5$ and FAPO-5. They agree with those of $AlPO_4$-5 and FAPO-5 published in the literature (*16, 17*). Both the peak position and the intensity of FAPO-5 were quite similar to those of $AlPO_4$-5. After the calcination, however, there was a slight change in the relative peak intensities. The XRD patterns did not reveal any minor

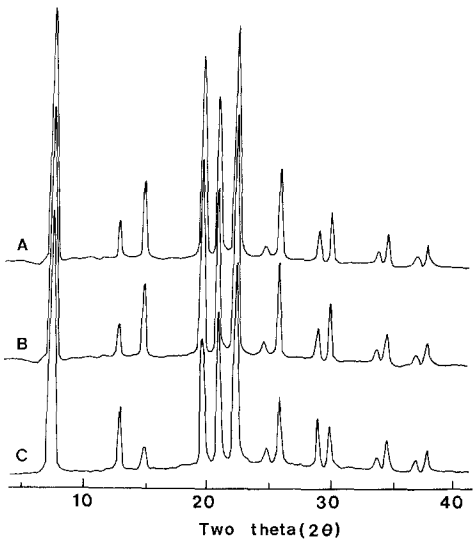

FIG. 1. XRD patterns of (A) as-synthesized $AlPO_4$-5 (F0), (B) as-synthesized FAPO-5 (F4), and (C) calcined F4.

phase in either as-synthesized or calcined forms. Also, the crystal structure of FAPO-5 was thermally stable up to 1000 K. The color of the three as-synthesized samples (F1, F2, and F3) was white, while F4 was light tan. After the calcination, the color of the F3 sample changed from white to off-white.

Figure 2 shows the scanning electron micrographs of FAPO-5(F4). All samples are homogeneous and consist of spherical aggregates with diameter of 30–40 μm and composed of small plates.

Chemical composition and sorption capacities of the samples are summarized in Table 1. The sorption capacity and the uptake rate of 1,3,5-trimethylbenzene (TMB) decreased slightly with increasing iron content, as shown in Fig. 3 and Table 1. Elemental analysis showed that the at.% of Fe + Al nearly equaled that of P for all FAPO-5 samples. The surface concentration of iron in samples F1 and F2 was similar to that of the bulk. A slight enrichment of iron at the surface was observed in F3 and F4 samples.

Figures 4(B) and (C) show the photoacoustic spectra of as-synthesized and cal-

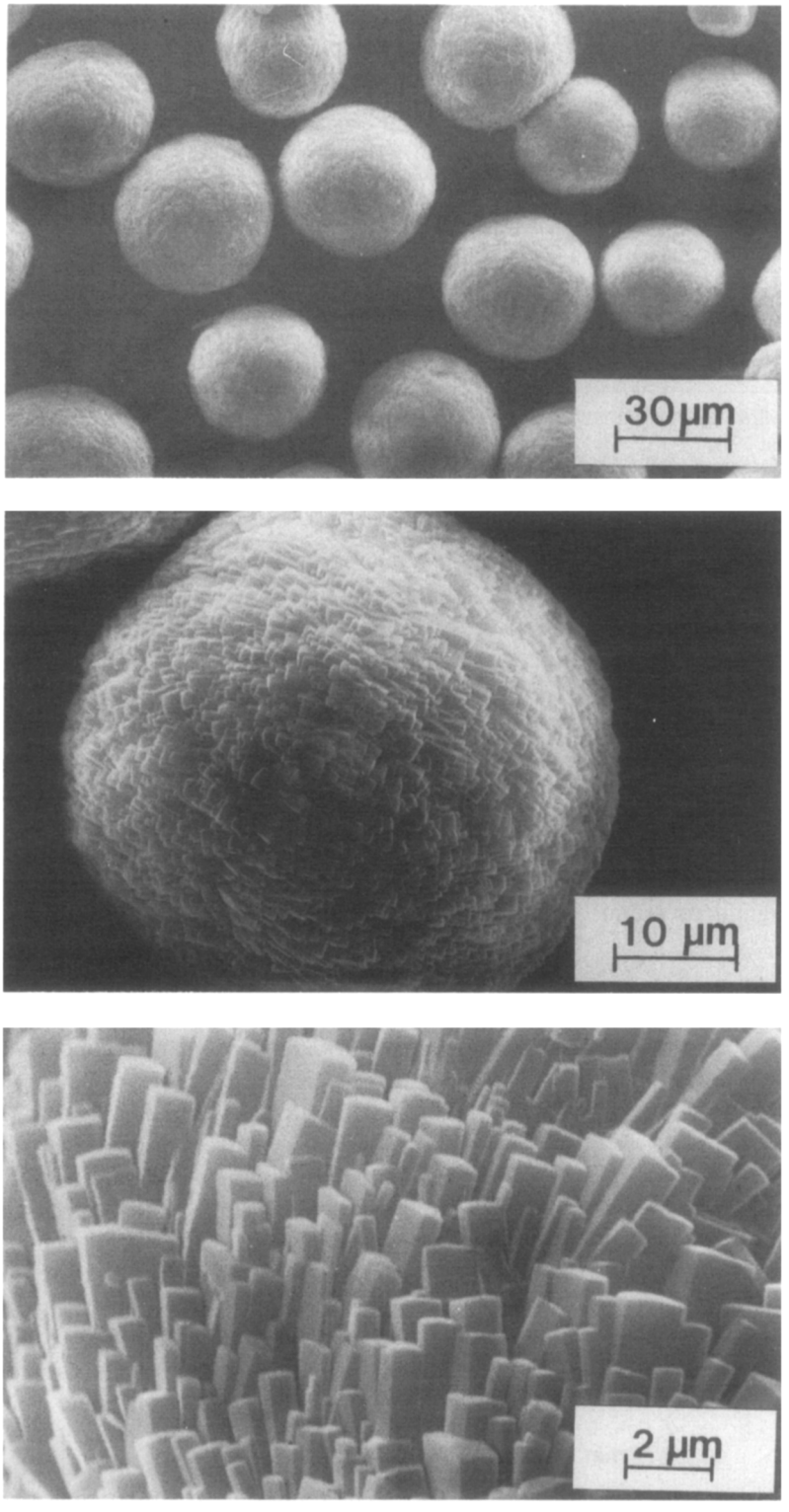

FIG. 2. Scanning electron micrographs of FAPO-5 (F4).

TABLE 1

Elemental Analysis and Sorption Capacities of $AlPO_4$-5 and FAPO-5 Samples

Sample	Composition (atomic %)						Sorption Capacity (mmol/g)[a]			
	Bulk			Surface[a]			Nitrogen[b]	*n*-Hexane[c]	Benzene[c]	1,3,5-TMB[d]
	Fe	Al	P	Fe	Al	P				
F0		51.0	49.0				4.82	1.08	1.32	0.80
F1	0.9	49.6	49.5	0.8	49.4	49.8	4.90	1.13	1.39	0.83
F2	1.8	48.2	50.0	1.6	48.5	49.9	4.94	1.10	1.35	0.74
F3	2.2	47.1	50.7	2.8	48.2	49.0	4.83	1.04	1.35	0.73
F4	3.1	47.0	49.9	3.9	46.8	49.3	4.69	0.98	1.30	0.69

[a] Calcined in flowing nitrogen at 780 K, followed by air at 780 K.
[b] $P/P_0 = 0.4$ at 77 K.
[c] $P/P_0 = 0.4$ at 295 K.
[d] $P_0 = 30$ Torr at 363 K.

cined FAPO-5's, respectively, in the visible region. For comparison, the spectra of Fe-silicate ZSM-5 are shown in Fig. 4(A). The as-synthesized Fe-silicate ZSM-5 showed four weak but apparent bands at about 375, 410, 435, and 480 nm which were assigned to Fe(III) surrounded tetrahedrally by oxygen (*5, 8, 29, 30*). After the calcination in air, the background level was increased up to 10-fold compared to that of the as-synthesized form. The ligand to metal charge-transfer (CT) band became too strong to clearly determine the resolution of all transition bands.

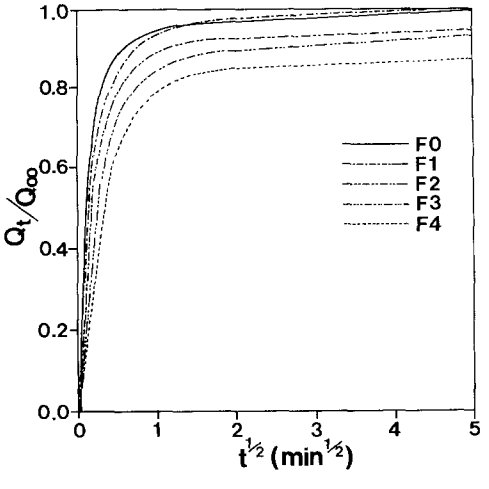

FIG. 3. Dependence of sorption kinetics of 1,3,5-trimethyl benzene (TMB) at 363 K on Fe content.

The spectra of all FAPO-5 samples exhibited different patterns from that of Fe-silicate ZSM-5. The spectra of as-synthesized FAPO-5 samples showed a band around 425 nm, while in F1 and F2 a band around 380 nm was observable as a shoulder. With increasing iron content there was an increase in the intensity of both the CT band and the 425 nm band. All calcined FAPO-5 samples showed spectra of four well resolved bands at about 380, 410, 435, and 480 nm, similar to that of as-synthesized Fe-silicate ZSM-5.

Figures 5 (A) and (B) show the effect of thermal treatments and hydration, respectively, on the PA spectra of the FAPO-5 samples. When the as-synthesized F2 was treated in flowing helium at 620 K, all transition bands were obscured by the CT band. When it was heated further to 770 K in helium, no peak could be observed due to strong absorption by black residue not fully removed. After the sample was treated in air at 800 K for 5 hr the PA spectra of four clearly resolved bands could be observed. The reductive treatment in flowing H_2 at 800 K for 24 hr did not affect the above four

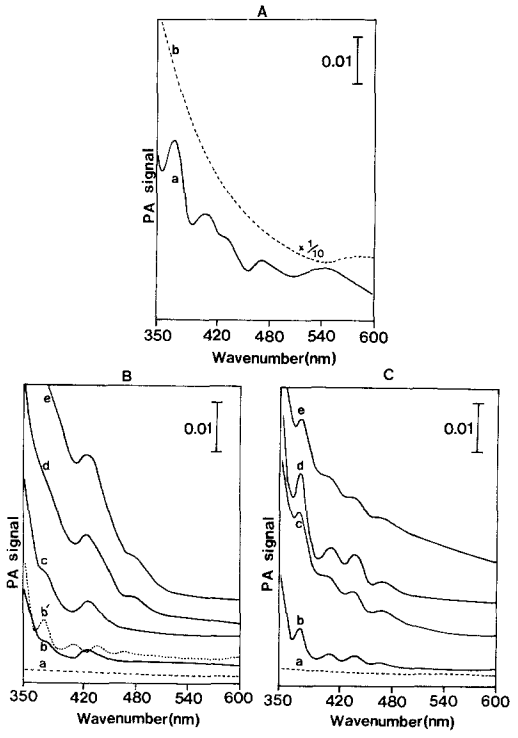

FIG. 4. PA spectra of (A) Fe-Silicate ZSM-5, (B) as-synthesized FAPO-5s, and (C) calcined FAPO-5s. (A): (a) as-synthesized; (b) calcined. (B) as-synthesized (a) F0; (b) F1; (c) F2; (d) F3; (e) F4; (b') calcined F1 for clarity comparison of spectra. (C) calcined FAPO-5s, (a)–(e) same as (B).

transition bands. But exposure of the calcined F3 sample to water vapor resulted in the gradual disappearance of the four transition bands and the appearance of a 425 nm band. The PA spectra obtained were similar to those of the as-synthesized F3 sample.

Figure 6 shows the EPR spectra of as-synthesized FAPO-5's taken at 77 K after the samples were dried in air at 400 K. All of the as-synthesized FAPO-5 samples showed the resonance absorptions around $g = 4.3$ and $g = 2.0$, except for the difference both in peak height (H) and peak-to-peak line width (H_{p-p}). The intensity of the $g = 4.3$ signal ($H_{p-p} = 95$ G) leveled off at F2, whereas that of the $g = 2.0$ signal increased rather linearly with increasing iron content (H_{p-p} increased from 150 G (F1) to 400 G (F4)). When the recording temperature was lowered from 298 to 77 K, the increase in the intensity of the $g = 4.3$ signal was 2.5–3-fold larger than that of the $g = 2.0$ signal.

Figure 7 shows the effect of various treatments on the EPR spectra of the calcined, dehydrated sample (F2). When the calcined sample was treated under the severe reductive condition in flowing H_2 at 780 K for 2 days, no changes were observed in the EPR spectra. Exposure of the calcined sample to water vapor, however, resulted in an increase in the intensity of the $g = 4.3$ signal, while that of the $g = 2.0$ signal decreased. The EPR spectra obtained after the treatment were similar to those of the as-synthesized F2 sample. In the case of Fe-silicate ZSM-5, the decrease in the intensity of the $g = 4.3$ signal was observed after the calcination (*3*). When the calcined Fe-silicate ZSM-5 was exposed to water vapor, the intensity of the $g = 2.0$ signal increased without any effect on the intensity of the $g = 4.3$ signal, and the signal decreased upon evacuation. When the calcined F2 sample was exposed to ammonia vapor, a new $g = 6.0$ signal appeared. When the F2 sample saturated with ammonia vapor was evacuated at room temperature, the $g = 6.0$ signal reappeared, while the intensity of the $g = 2.0$ signal decreased. The original EPR spectrum of the calcined sample could be restored after the sample was heated to 430 K in vacuum for 1 hr.

Figure 8 shows the DTG results obtained in flowing air. The TEAOH-$AlPO_4$-5 sample showed two stages of weight loss, one around 320–400 K and the other around 570–620 K. The first stage of weight loss is due to the desorption of physically adsorbed water. The second stage of weight loss is probably due to the oxidative decomposition of occluded TEAOH. In the case of TEAOH-FAPO-5, there was an additional weight loss at about 710 K. The number of the templating agent obtained from the weight loss per unit cell is given in Table 2. It is one both for the $AlPO_4$-5 and the FAPO-5 samples.

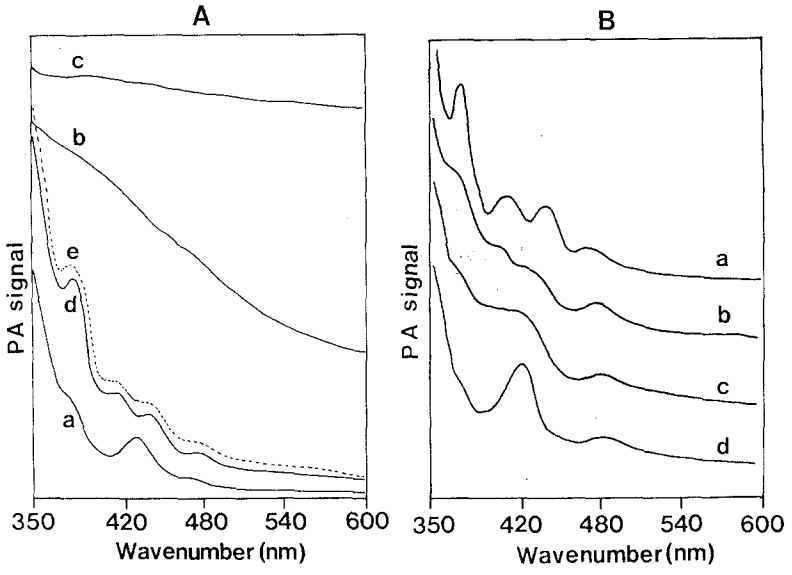

FIG. 5. PA spectra of FAPO-5 on thermal (A) and hydration (B) treatment. (A): (a) as-synthesized F2; (b) activated at 620 K in helium atmosphere for 6 hr; (c) activated at 770 K for 3 hr; (d) activated in air at 800 K for 5 hr; (e) treated in flowing hydrogen for the sample (d) at 800 K for 24 hr. (B): (a) calcined, dehydrated F3; (b) exposed to water vapor for 3 hr; (c) exposed to water vapor for 9 hr; (d) exposed to water vapor overnight.

Figure 9 shows the DSC results of the as-synthesized $AlPO_4$-5 and FAPO-5 samples in air atmosphere. There are two peaks, one around 570–620 K and the other around 700–750 K, associated with the decomposition of templates. Only one peak (570–620 K) was observed for the $AlPO_4$-5 sample, whereas both peaks were observed for FAPO-5 samples.

Figure 10 shows the changes in nitrogen surface area with increasing calcination temperature. No change in the surface area was observed for the first stage (470 K) in all samples. The surface area increased in the second stage of thermal treatment (470–620 K), but the amount of increase became progressively less with increasing iron content. After the third stage (620–770 K), the surface area of the FAPO-5 samples became comparable to that of $AlPO_4$-5. These results are consistent with the TG/DSC results.

Figure 11 shows the TPDE/MS spectra of TEAOH-$AlPO_4$-5 (F0) and TEAOH-FAPO-

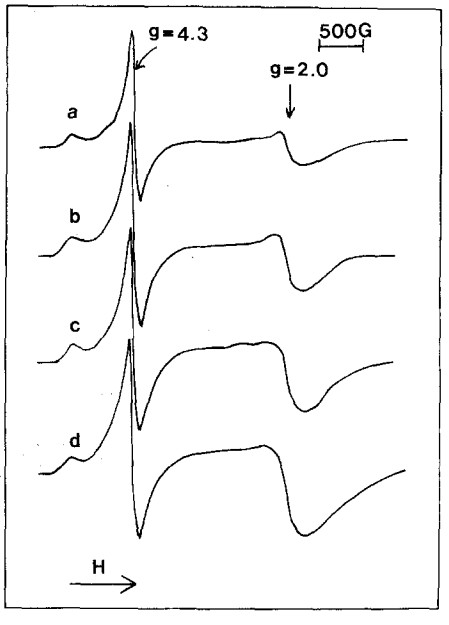

FIG. 6. EPR spectra of as-synthesized FAPO-5s: (a) F1; (b) F2; (c) F3; (d) F4.

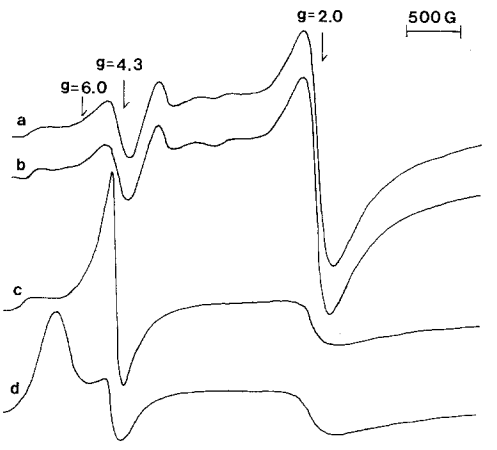

FIG. 7. EPR spectra of F2 on the various treatments: (a) calcined, fully evacuated; (b) treated with H_2 at 770 K for 2 days; (c) exposed to water vapor overnight for (a); (d) exposed to ammonia vapor (300 Torr) for 30 min, followed by vacuum evacuation at room temperature overnight.

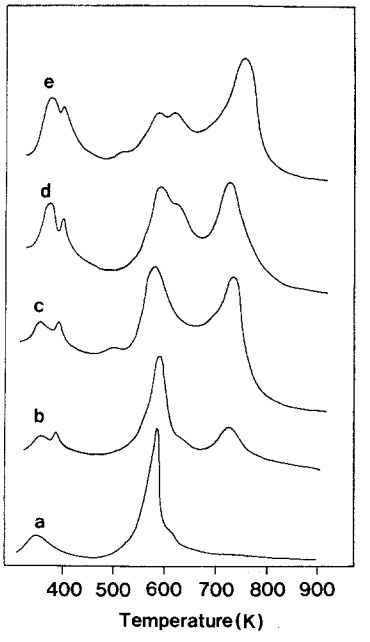

FIG. 8. DTG curves of as-synthesized $AlPO_4$-5 and FAPO-5s: (a) F0; (b) F1; (c) F2; (d) F3; (e) F4.

5 (F4). In $AlPO_4$-5, the template decomposed mainly into ethylene, water, and triethyl-amine in the temperature range where DTG and DSC peaks were observed. Formation of a small amount of diethylamine was also observed. The mass chromatogram of the decomposed products from FAPO-5 was different from that of $AlPO_4$-5. In the case of FAPO-5, the appearance of an ethylene peak and a considerable increase in butene formation were observed in the high temperature region where the second DTG and DSC peaks were observed. The noticeable difference in the decomposition pattern between $AlPO_4$-5 and FAPO-5 was the formation of aromatic compounds such as toluene, xylene, and trimethylbenzene in FAPO-5.

DISCUSSION

The FAPO-5 materials synthesized with Fe(II) and TEAOH and differing in iron content were characterized by using various physicochemical methods to elucidate the incorporation of the iron ions into the aluminophosphate matrix.

The iron in as-synthesized FAPO-5 may have both oxidation states Fe(III) and Fe(II) in the framework or nonframework of FAPO-5, although the sample is prepared with an Fe(II) source, due to the oxidation of some of the Fe(II) ions during the gel preparation (*12–14*).

It is difficult to observe the very weak, spin-forbidden *d–d* transition bands of Fe(III) ions obscured by the charge transfer band. But, in general, the electronic spectra

TABLE 2

Thermogravimetric Analysis of $AlPO_4$-5 and FAPO-5 Samples

Sample	Weight loss (%)		Total (%)	Template/U.C
	530–650 K	650–770 K		
F0	9.17		9.17	1.03
F1	6.57	2.66	9.23	1.06
F2	4.94	4.34	9.28	1.08
F3	4.52	4.73	9.25	1.08
F4	3.64	5.60	9.24	1.06

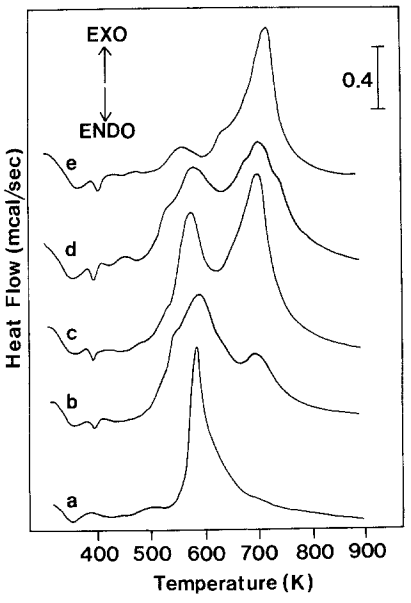

FIG. 9. DSC profile of as-synthesized $AlPO_4$-5 and FAPO-5s: (a) F0; (b) F1; (c) F2; (d) F3; (e) F4.

of Fe(III) ions having tetrahedral symmetry give a characteristic *d–d* transition in the visible region similar to that observed in as-synthesized Fe-silicate ZSM-5, while Fe(III) ions having octahedral symmetry give one absorption band around 410–430 nm, observed in iron-containing phosphate glass (*31*) and pillared clay (*32*) materials. ^{27}Al-NMR studies have shown that in some of the $AlPO_4$ molecular sieves a substantial secondary coordination of a certain framework Al(III) site may occur with water molecules entrapped within the channel system, and also rehydration of the calcined $AlPO_4$ results in the symmetry change of a certain framework tetrahedral Al(III) to pseudo-octahedral Al(III) (*33–36*). The observation that the intensity of the band around 425 nm increased with increasing iron content of the FAPO-5 samples suggests that this band may be related to the octahedral Fe(III) ions. The spectra due to the framework Fe(III) ions having tetrahedral symmetry were obscured by the band due to the octahedral Fe(III) ions, but the shoulder band at 380 nm in as-synthesized FAPO-5 clearly indicates the presence of spectra due to the tetrahedral Fe(III) ions.

The fact that the intensity of the bands due to tetrahedral Fe(III) ions in the spectra of calcined FAPO-5 samples was high and the spectra were well resolved compared to those of as-synthesized FAPO-5, and that these transition bands were not affected by a severe reductive treatment, indicate that Fe(II) ions located in the framework position are oxidized to Fe(III) ions while remaining in the framework position.

Hydration of the calcined FAPO resulted in a gradual change of the spectra due to tetrahedral Fe(III) ions to that of octahedral Fe(III) ions (425 nm) similar to that observed for as-synthesized FAPO-5. These facts suggest that the 425 nm band may be attributed to pseudo-octahedral Fe(III) ions in the framework similar to the pseudo-octahedral framework Al(III) in $AlPO_4$ materials.

The results of EPR seemed to be in line with the results of PAS. The EPR pattern of calcined, hydrated FAPO-5 was similar to that of as-synthesized FAPO-5. The reversible change of some of the $g = 2.0$ signal to the $g = 4.3$ signal upon hydration for cal-

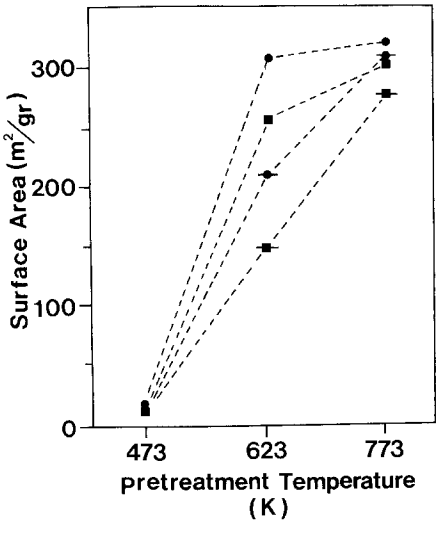

FIG. 10. Change of nitrogen surface area on thermal treatment: (●) FO; (■) F1; (●) F2; (■) F4.

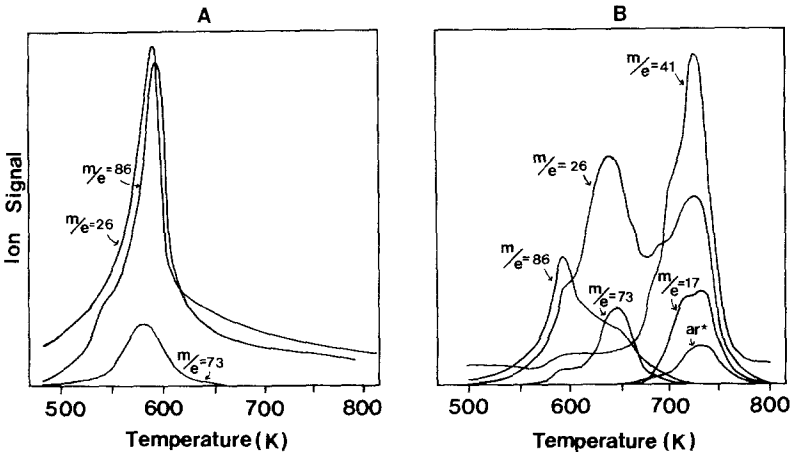

FIG. 11. TPDE/MS spectra of (A) as-synthesized $AlPO_4$-5(F0) and (B) as-synthesized FAPO-5 (F4). The ion signals represent the following: *m/e* = 26 (ethylene), *m/e* = 86 (triethylamine), *m/e* = 73 (Diethylamine), *m/e* = 41 (butene), and *m/e* = 17 (ammonia); ar*, which represents the aromatic compounds, is the combination of *m/e* = 92, 106, and 120.

cined FAPO-5 is apparently different from the case of Fe-silicate ZSM-5, in which the $g = 2.0$ signal was increased by hydration without any effect on the $g = 4.3$ signal. An isotropic $g = 2.0$ signal is attributed to the Fe(III) ions in a rather symmetrical environment (*8, 23, 26*). In the iron phosphate $FePO_4$ system where Fe(III) ions are located in a tetrahedral environment, only the $g = 2.0$ signal is observed (*8*), and this suggests that the $g = 2.0$ signal may be assigned to the tetrahedral Fe(III) ions in calcined FAPO-5 samples. There is some disagreement over the assignment of the EPR signal with $g = 4.3$. The $g = 4.3$ signal can arise from distorted tetrahedral or octahedral Fe(III) ions depending on the ligand distortion, although the presence of this signal is considered as one indication of the incorporation of Fe(III) ions into the tetrahedral framework in a zeolite system (*3, 22–28*). Considering the PAS results, it seems appropriate to assign the $g = 4.3$ signal observed both in as-synthesized and rehydrated FAPO-5 to pseudo-octahedral Fe(III) ions in the framework.

The results of PAS and EPR indicate that a large portion of Fe(III) ions are located in the framework position of $AlPO_4$-5 both tetrahedrally and pseudo-octahedrally in the as-synthesized form, and even after the calcination a substantial portion of Fe(III) ions remained in the framework position having tetrahedral symmetry.

It is known that the organic base such as TEAOH used in the synthesis of zeolite is present at least in two types of tetraethylammonium ions; one is TEAOH, which is less strongly bound to the surface, and the other is TEA^+ ion acting as a charge balancing cation if any acidic sites are present (*13, 21, 37, 38*).

Results of the thermal analysis of as-synthesized $AlPO_4$-5 and FAPO-5 samples suggest the presence of two different template species.

Thermal analysis of as-synthesized $AlPO_4$-5 and FAPO-5 samples by DTG and DSC showed that there are two peaks, one around 570–620 K and the other around 700–750 K, associated with the decomposition of templates. For the $AlPO_4$-5 sample, only one peak around 570–620 K was observed. For FAPO-5 samples, both peaks were present, and the intensity of the high temperature peak increased with increasing

iron content. The thermal decomposition pattern of the templates in $AlPO_4$-5 and FAPO-5 studied by TPDE/MS was also different. For FAPO-5 samples, the formation of acid-catalyzed product was observed in the temperature range where high temperature DTG and DSC peaks were observed. Parker *et al.* observed similar results in the decomposition of TEA^+ ions in Al(III)-substituted silicate ZSM-5 (*21*).

It seemed that in the course of synthesis, Fe(II) ions are introduced into the framework in place of Al(III) ions in the form of Fe(II) TEA^+ together with Fe(III) ions. Here the template seemingly served both as the templating agent and the charge compensating agent (*13, 38*).

After the calcination, these framework Fe(II) ions in FAPO-5 samples seemed to be oxidized to Fe(III) ions and remain in the framework position having tetrahedral symmetry. In the case of Fe-silicate ZSM-5, however, some of the Fe(III) ions in the framework seemed to be removed after the calcination.

In calcined FAPO-5, adsorption of ammonia resulted in the appearance of a new signal with $g = 6.0$. The species responsible for the $g = 6.0$ signal are not clear, but Loveridge and Parke showed that in amber glasses Fe(III) ions surrounded by three oxygen and one sulfur in a tetrahedral arrangement would give $g = 6$ resonance (*23*). Also, Castner *et al.* showed that tetrahedra with one of the ligands different from the other three would give absorption at $g = 6$ (*24*).

REFERENCES

1. Szostak, R., "Molecular Sieves: Principles of Synthesis and Identification," p. 205. Van Nostrand–Reinhold, New York, 1989.
2. Flanigen, E. M., Lok, B. M., Patton, R. L., and Wilson, S. T., *in* "Proceedings of the 7th International Zeolite Conference" (Y. Murakami, A. Lijimi, and J. W. Ward, Eds.), p. 103. Kodansha, Tokyo, 1986.
3. Szostak, R., and Thomas, T. L., *J. Catal.* **100,** 555 (1986).
4. Szostak, R., Nair, V., and Thomas, T. L., *J. Chem. Soc., Faraday Trans. 1* **83,** 487 (1987).
5. Iton, L. E., Beal, R. B., and Hodul, D. T., *J. Mol. Catal.* **21,** 151 (1983).
6. Kustov, L. M., Kazansky, V. B., and Ratnasamy, P., *Zeolites* **7,** 79 (1987).
7. Borade, R. B., *Zeolites* **7,** 398 (1987).
8. Lin, D. H., Coudurier, G., and Vedrine, J. C., *in* "Zeolites; Facts, Figures, Future" (P. A. Jacobs and R. A. Van Santen, Eds.), p. 227. Elsevier, Amsterdam, 1989.
9. Kumar, R., and Ratnasamy, P., *J. Catal.* **121,** 89 (1990).
10. Kumar, R., Thangaraj, A., Bhat, R. N., and Ratnasamy, P., *Zeolites* **10,** 85 (1990).
11. Ratnasamy, P., Kotasthane, A. N., Shiralkar, V. P., Thangara, A., and Ganapathy, S., *ACS Symp. Ser.* **398,** 405 (1989).
12. Cardile, C. M., Tapp, N. J., and Milestone, N. B., *Zeolites* **10,** 90 (1990).
13. (*a*) Li, H. X., Martens, J. A., Jacobs, P. A., Schubert, S., Schmidts, F., Ziethen, H. M., and Trautwein, A. X., *in* "Innovation in Zeolite Materials Science" (P. J. Grobet, W. J. Mortier, E. F. Vansant, and G. Schulz-Ekloff, Eds.), p. 75. Elsevier, Amsterdam, 1988; (*b*) Li, H. X., Martens, J. A., Jacobs, P. A., Schubert, S., Schmidts, F., Ziethen, H. M., and Trautwein, A. X., *in* "Zeolites as Catalysts, Sorbents, and Detergent Builders: Application and Innovations" (H. G. Karge, and J. Weitkamp, Eds.), p. 735. Elsevier, Amsterdam, 1989.
14. Ojo, A. F., Dwyer, J., and Parish, R. V., *in* "Zeolites: Facts, Figures, Future" (P. A. Jacobs and R. A. Van Santen, Eds.), p. 227. Elsevier, Amsterdam, 1989.
15. Wenqin, P., Shilun, Q., Qiubin, K., Zhiyun, W., Shaoyi, P., Guochuan, F., and Di, T., *in* "Zeolites: Facts, Figures, Future" (P. A. Jacobs and R. A. Van Santen, Eds.), p. 281. Elsevier, Amsterdam, 1989.
16. Messina, C. A., Lok, B. M., and Flanigen, E. M., U.S. Patent, 4,554,113 (1985).
17. Wilson, S. T., Lok, B. M., and Flanigen, E. M., U.S. Patent, 4,310,440 (1982).
18. Rabo, J. A., Pellet, R. J., Coughlin, P. K., and Shamshoum, E. S., *in* "Zeolites as Catalysts, Sorbents, and Detergent Builders: Applications and Innovations" (H. G. Karge, and J. Weitkamp, Eds.), p. 1. Elsevier, Amsterdam, 1989.
19. Chon, H., and Park, D. H., *J. Catal.* **114,** 1 (1988).
20. Lee, K. Y., and Chon, H., *J. Catal.* **126,** 677 (1990).
21. Parker, L. M., Bibby, D. M., and Patterson, J. E., *Zeolites* **4,** 168 (1984).
22. Griffith, J. S., *Mol. Phys.* **8,** 213 (1964).
23. Loveridge, D., and Parke, S., *Phys. Chem. Glasses* **12,** 19 (1971).
24. Castner, T., Newell, G. S., Holton, W. C., and Slichter, C. P., *J. Chem. Phys.* **32,** 668 (1960).
25. McNicole, B. D., and Pott, G. T., *J. Catal.* **25,** 223 (1972).
26. Derouane, E. G., Mestdagh, M., and Vielvoye, L., *J. Catal.* **33,** 169 (1974).

27. Evmiridis, N. P., *Inorg. Chem.* **25,** 4362 (1986).
28. Wichterliva, B., *Zeolites* **1,** 181 (1981).
29. Fox, K. E., Furukawa, T., and White, W. B., *Phys. Chem. Glasses* **23,** 169 (1982).
30. Edwards, R. J., Paul, A., and Douglas, R. W., *Phys. Chem. Glasses* **13,** 131 (1972).
31. Kurkijan, C. R., and Sigety, E. A., *Phys. Chem. Glasses* **9,** 73 (1968).
32. Kostapapas, A., Suib, S. L., Coughlin, R. W., and Occelli, M. L., *in* "Zeolites; Facts, Figures, Future" (P. A. Jacobs and R. A. Van Santen, Eds.), p. 399. Elsevier, Amsterdam, 1989.
33. Blackwell, C. S., and Patton, R. L., *J. Phys. Chem.* **88,** 6135 (1984).
34. Blackwell, C. S., and Patton, R. L., *J. Phys. Chem.* **92,** 3965 (1988).
35. Goepper, M., Guth, F., Delmotte, L., Guth, J. L., and Kessler, H., *in* "Zeolites: Facts, Figures, Future" (P. A. Jacobs and R. A. Van Santen, Eds.), p. 857, Elsevier, Amsterdam, 1989.
36. Wu, Y., Chmellka, B. F., Pines, A., Davis, M. E., Grobet, P. J., and Jacobs, P. A., *Nature (London)* **346,** 550 (1990).
37. Perez-Pariente, J., Martens, J. A., and Jacobs, P. A., *Appl. Catal.* **31,** 35 (1987).
38. Flanigen, E. M., Patton, R. L., and Wilson, S. T., *in* "Innovation in Zeolite Materials Science" (P. J. Grobet, W. J. Mortier, E. F. Vansant, and G. Schultz-Ekloff, Eds.), p. 13. Elsevier, Amsterdam, 1988.